MATHEMATICAL MODEL IMPROVEMENT FOR THE NONLINEAR CHARACTERISTICS OF TRANSONIC FLUTTER

Keiichi Imamura*
***Department of Mechanical Engineering,**
University of Fukui, Fukui, Japan

Keywords: *Aeroelasticity, transonic flutter, LCO*

Abstract

In order to make better agreement with transonic wind tunnel experimental data, which was obtained in the Japan Aerospace Exploration Agency (JAXA) in 1990's, we proposed new mathematical model to improve the previous model. The bifurcation diagram was analyzed by a continuation method. The continuation method can continuously follow the solutions of dynamical system, such as a limit cycle oscillation (LCO), as one or more parameters in the systems are changed. So the continuation method enables to analyze the bifurcation diagram efficiently even through an unstable limit cycle (stability boundary) and can obtain a saddle-node point. We first analyzed the bending dominant (first) mode model and the torsion dominant (second) mode model separately, then combined the two models into one model. The final adjustment of the free parameters was performed to get the improved model. The model has a fourth order nonlinearity in the velocity of the first mode and the deflection of the second mode.

1 Introduction

Flutter is self-excited oscillation, which occurs due to interaction among aerodynamic force, elastic force and inertial forces of structures. In the transonic region, the flutter dynamic pressure falls rapidly; a phenomenon called transonic dip. Transonic flutter around a transonic dip often behaves like a limit cycle oscillation (LCO). The feature of transonic flutter differs from typical flutter in that it repeats fixed amplitude and fixed period oscillation. It can be attributed to a separation of the airflow associated with shock waves propagating along the surface of the wing [1-3].

Matsushita proposed the nonlinear mathematical model [4], in which oscillating modes originally incorporated into a nonlinear mathematical model are the first and second modes. The model corresponds with wind tunnel test results qualitatively. In the following Chapter 2 of this paper, I describe a wing model and the results of transonic wind tunnel tests. In Chapter 3, I describe the previous nonlinear mathematical model and in Chapter 4, a newly improved mathematical model will be analyzed. In Chapter 5, I describe the trial extension to four-mode model. Throughout the present paper, I analyze the bifurcation characteristics of the mathematical model using a continuation method.

2 Wing Model and Results of Transonic Wind Tunnel Tests

Figure 1 is a wing model used in transonic wind tunnel tests in JAXA. This wing model is a scale-down model of a civil aircraft's wing which has a high aspect ratio. The wing model has a wing span of 1043 mm, a wing code of 369 mm at a wing root, 101 mm at a wing tip and a sweepback angle of 16.9 deg. In this wing model, a leading edge control surface was used in order to apply oscillatory disturbance to this wing model. The wing response is measured by the accelerometer. A typical result of the transonic wind tunnel tests is shown in Fig. 2.

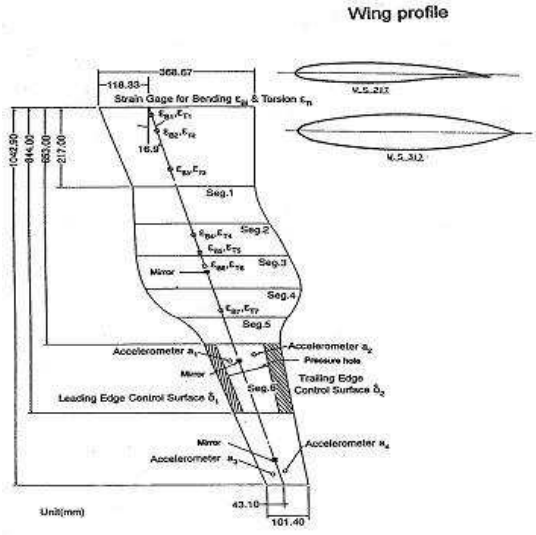

Fig. 1 High aspect ratio wing model.

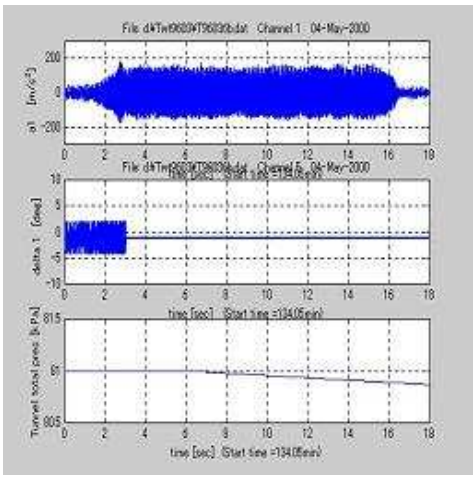

Fig. 2 Saddle-node bifurcation phenomenon due to quasi-static decrease of a wind tunnel dynamic pressure.

In this figure from the top chart to the bottom, an output of accelerometer, a deflection of a leading edge and a dynamic pressure in transonic wind tunnel are shown, respectively. As you can see at the top chart, LCO suddenly stops when the dynamic pressure goes down at a certain level. Collecting all the experimental data obtained in transonic wind tunnel tests, we can get an experimental bifurcation diagram as shown in Fig. 3. In Fig. 3, a vertical axis shows LCO amplitude and a horizontal axis shows dynamic pressure. A point of ● and ∗ denotes LCO's amplitude and stability boundary, respectively.

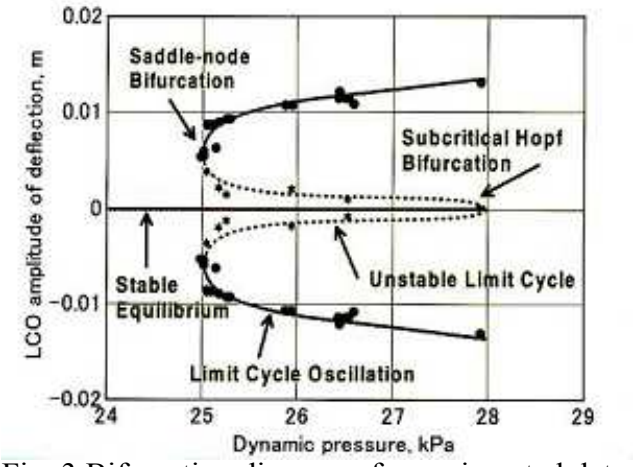

Fig. 3 Bifurcation diagram of experimented data.

3 Previous Nonlinear Mathematical Model for Two Modes

For completeness of the discussion, let's review the previous math model. The linear finite state equation for two modes flutter can be expressed as the following equation [4],

$$\dot{x} = Ax \;\; ; \quad x = [q, \dot{q}, z]^T \in R^6 \tag{1}$$

$$A = \begin{bmatrix} 0 & I & 0 \\ -(M-A_2)^{-1}(K-A_0) & -(M-A_2)^{-1}(C-A_1) & -(M-A_2)^{-1} \\ B_0 & 0 & \Lambda \end{bmatrix} \in R^{6*6} \tag{2}$$

where $q(t)$ is a vector of generalized coordinates for two modes, z is an augmented variable expressing aerodynamic delay, M, B_c , and K are the mass, the structural damping, and the stiffness matrices, respectively. A_0, A_1, A_2, B_0 and Λ are coefficient matrixes of a finite state aerodynamic model. The nonlinear mathematical model can then be constructed by introducing the nonlinear terms in the damping terms as,

$$\dot{x} = (A + \Delta A_{NL})x \tag{3}$$

where nonlinear coefficients ΔA_{NL} has the following components.

$$\Delta A_{NL} = \begin{bmatrix} 0 & 0 & 0 \\ 0 & (M-A_2)^{-1}\Delta A_{INL} & 0 \\ 0 & 0 & 0 \end{bmatrix} \in R^{6*6} \tag{4}$$

At the aerodynamic force damping term, $(M - A_0)^{-1}\Delta A_{NL}$, diagonal element has the fourth order nonlinear term such as,

$$\Delta \boldsymbol{A}_{INL} = \begin{bmatrix} \left(\beta_1 q_1^{\,2} + \gamma_1 q_1^{\,4}\right) a_{11a} & 0 \\ 0 & \left(\beta_2 q_2^{\,2} + \gamma_2 q_2^{\,4}\right) a_{22a} \end{bmatrix} \quad (5)$$

where a_{11a} and a_{22a} are the aerodynamic part of the coefficients for the bending dominant (first) mode and the torsion dominant (second) mode, respectively. Parameters β_i and γ_i are free parameters, which are to be determined to fit the transonic wind tunnel test data. Fig. 4 shows the bifurcation diagram of LCO for this model. Discrepancy still exists in the stability boundary as shown in Fig. 4. Bifurcation analysis was done by using a continuation method.

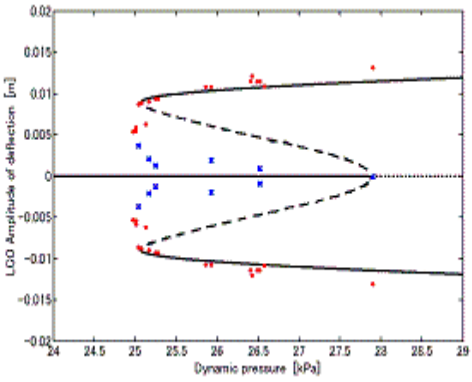

Fig. 4 Bifurcation diagram of analysis of the previous two-mode model.

In Fig. 4, test data are also plotted with mark ● and ×. Solid line and dotted line are results of analysis for the previous mathematical model.

4 Improvement of the Previous Two-Mode Model

In order to improve the nonlinear mathematical model, we analyze the first mode and the second mode separately. In the fourth order nonlinear coefficient of a_{11a}, the generalized coordinate q_1 is replaced with $\dot{q}_1$ (the velocity q_1), i.e., $\beta q_1^{\,2} + \gamma q_1^{\,4}$, was replaced with $\beta_1 \dot{q}_1^{\,2} + \gamma_1 \dot{q}_1^{\,4}$. Then the first mode model has the nonlinear term as

$$\Delta \boldsymbol{A}_{INL} = \begin{bmatrix} \left(\beta_1 \dot{q}_1^{\,2} + \gamma_1 \dot{q}_1^{\,4}\right) a_{11a} & 0 \\ 0 & 0 \end{bmatrix} \quad (6)$$

and the corresponding bifurcation diagram takes the form as shown at the center of Fig. 5 where the parameters β_1, γ_1 are set at the initial values. Fig. 5 shows over all how the bifurcation diagram is changing as β_1 and γ_1 change.

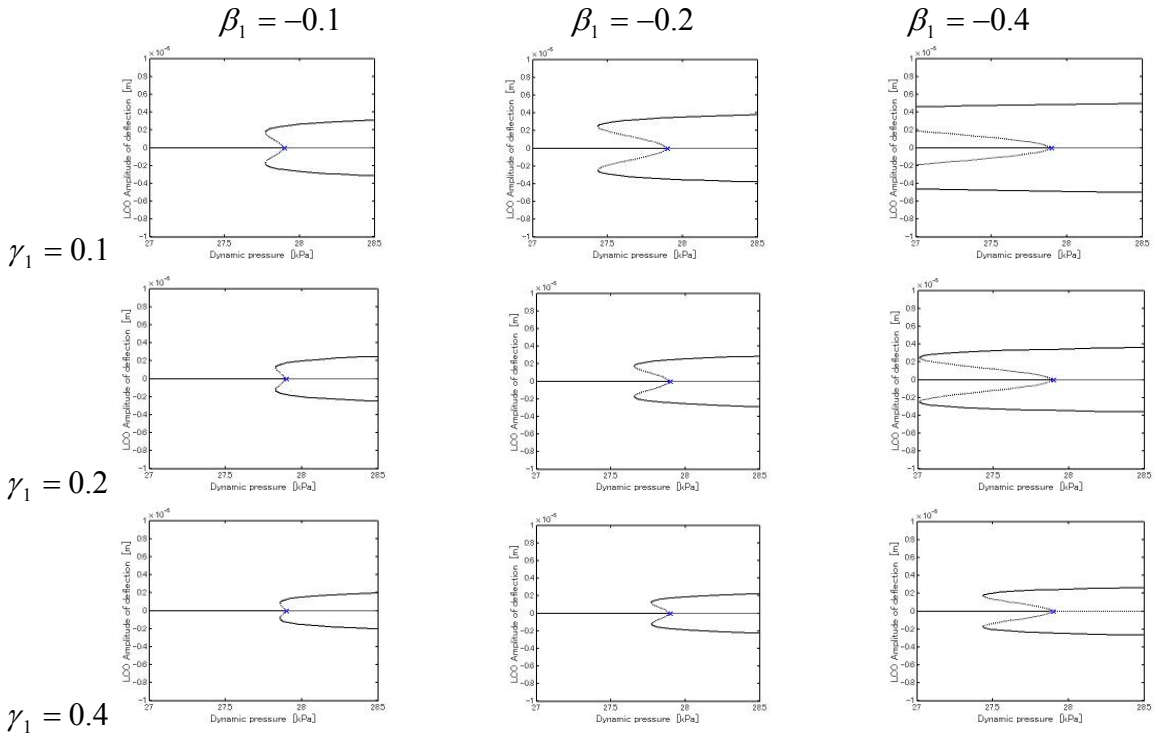

Fig. 5 Result of analysis of continuation method.

If β_1 is made small LCO amplitude becomes large, and saddle-node is extended to a lower speed domain, while if γ_1 is made small, there is the same tendency. It turns out that what is necessary is to make γ_1 small for increasing LCO amplitude, and just to increase β_1 a little, in order to keep a saddle-node with test data. However, when β_1 and γ_1 are changed at the same rate, there is a domain where it becomes impossible to analyze continuously by the continuation method. In order to make it in agreement with the test data, γ_1 should be made small and β_1 should also made small bit by bit. The final result in which the free parameters β_1 and γ_1 were chosen, so that the first mode model comes closer to the test, is shown in Fig. 6.

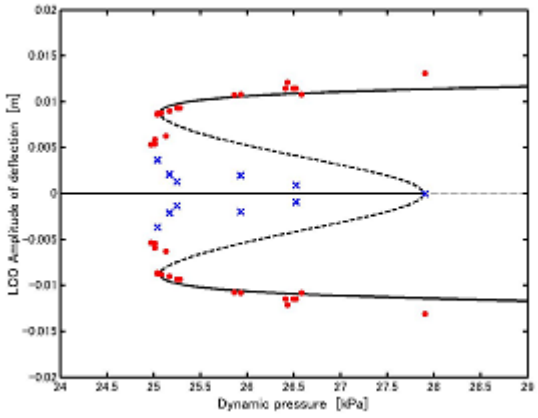

Fig. 6 Bifurcation diagram of analysis of the first mode.

It cannot be said that Fig. 6 is fully improved because one of a purpose of reducing a disagreement over stability boundary is not realized. So we have to introduce nonlinear term in the second mode. Regarding the second mode as a torsion dominant mode, I retain q_2 nonlinearity. The second mode model therefore has the following nonlinear term,

$$\Delta \boldsymbol{A}_{INL} = \begin{bmatrix} 0 & 0 \\ 0 & \left(\beta_2 q_2{}^2 + \gamma_2 q_2{}^4\right) a_{22a} \end{bmatrix} \qquad (7)$$

where corresponding bifurcation diagram takes the form as shown in Fig. 7.

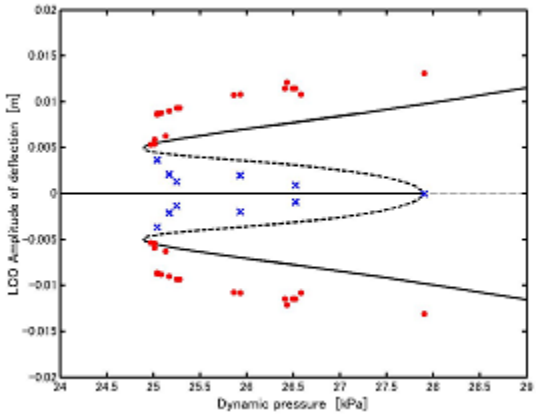

Fig. 7 Bifurcation diagram of analysis of the second mode.

The analysis method of Fig. 7 is the same as that of Fig. 6. This model improves stability boundary region, but it does not improve the amplitude of LCO. Therefore, we introduced the term, $\beta_1 \dot{q}_1^{\,2} + \gamma_1 \dot{q}_1^{\,4}$, in the first mode of the previous model and the term, $\beta_2 q_2^{\,2} + \gamma_2 q_2^{\,4}$, in the second mode. Combining the first and second mode model, we get the new mathematical model with the following nonlinear term.

$$\Delta \boldsymbol{A}_{INL} = \begin{bmatrix} \left(\beta_1 \dot{q}_1{}^2 + \gamma_1 \dot{q}_1{}^4\right) a_{11a} & 0 \\ 0 & \left(\beta_2 q_2{}^2 + \gamma_2 q_2{}^4\right) a_{22a} \end{bmatrix} \qquad (8)$$

Totally optimizing the four parameters β_1, γ_1, β_2, γ_2, I finally obtain the math model which has the bifurcation diagram shown in Fig. 8.

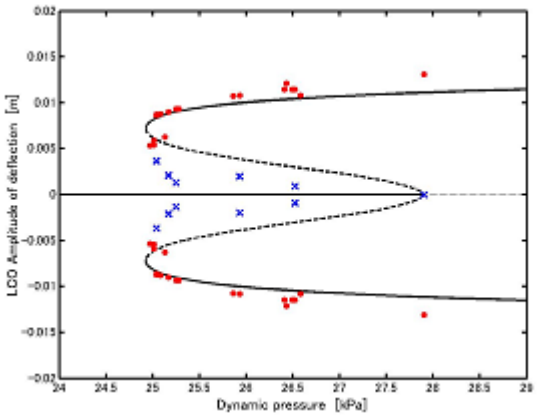

Fig. 8 Bifurcation diagram of analysis of the coupled mode.

Figure 8 is the result of the analytical bifurcation diagram made fit everywhere to the experiment

result, where the analytical diagram fit with the test data. I was able to improve the previous model particularly in the stability boundary region. The stability boundary previously shown in Fig. 4 comes closer to the experimental stability boundary as shown in Fig. 8. Though Fig. 8 still has a small discrepancy between the mathematical model and the test data, this discrepancy can be reasonably explained as follows. Disturbance in the wind tunnel flow or flow separation at the wing surface could reduce the stability region and could result in the discrepancy.

5 Trial Extension to Four-Mode Model

In Chapter 4, I analyzed the model only in consideration of simple first mode of bending and torsion. However, since higher order mode model is desirable in the accuracy of the model characteristics. So I analyze four-mode model as Chapter 4. As an extension of eq. (1) for two-mode model, the equation of four-mode model can be expressed by twelfth order model as shown below.

$$\dot{\boldsymbol{x}}(t)=\boldsymbol{A}\boldsymbol{x}(t);\ \boldsymbol{x}(t)=[\boldsymbol{q}(t)^T \quad \dot{\boldsymbol{q}}(t)^T \quad \boldsymbol{r}(t)^T]^T \in \boldsymbol{R}^{12\times 1} \tag{9}$$

$$\boldsymbol{A}=\begin{bmatrix} \boldsymbol{0} & \boldsymbol{I} & \boldsymbol{0} \\ \boldsymbol{A}_1 & \boldsymbol{A}_2 & \boldsymbol{A}_3 \\ \boldsymbol{B}_{0q} & \boldsymbol{0} & \boldsymbol{\Lambda} \end{bmatrix} \in \boldsymbol{R}^{12\times 12} \tag{10}$$

$$\boldsymbol{A}_1=-\boldsymbol{M}_q(\boldsymbol{K}-\boldsymbol{A}_{2q})\in\boldsymbol{R}^{4\times 4} \quad \boldsymbol{A}_2=-\boldsymbol{M}_q(\boldsymbol{B}_c-\boldsymbol{A}_{1q})\in\boldsymbol{R}^{4\times 4}$$

$$\boldsymbol{A}_3=\boldsymbol{M}_q\in\boldsymbol{R}^{4\times 4}$$

$$\boldsymbol{M}_q=(\boldsymbol{M}-\boldsymbol{A}_{0q})^{-1}\in\boldsymbol{R}^{4\times 4}$$

In this chapter, I use twelfth order nonlinear equation shown below.

$$\dot{\boldsymbol{x}}=\left(\boldsymbol{A}+\Delta\boldsymbol{A}_{NL}\right)\boldsymbol{x} \tag{11}$$

$$\Delta\boldsymbol{A}_{NL}=\begin{bmatrix} \boldsymbol{0} & \boldsymbol{0} & \boldsymbol{0} \\ \boldsymbol{0} & \boldsymbol{M}_q\boldsymbol{A}_{1q}\Delta\boldsymbol{A}_{INL} & \boldsymbol{0} \\ \boldsymbol{0} & \boldsymbol{0} & \boldsymbol{0} \end{bmatrix} \in \boldsymbol{R}^{12\times 12} \tag{12}$$

First of all, in order to analyze as Chapter 4, the nonlinear term is added to the first mode. The form of added nonlinear term is shown in eq. (13), and the result analyzed using this nonlinear term is shown in Fig. 9.

$$\Delta\boldsymbol{A}_{INL}=\begin{bmatrix} (\beta_1\dot{q}_1^2+\gamma_1\dot{q}_1^4) & 0 & 0 & 0 \\ 0 & 0 & 0 & 0 \\ 0 & 0 & 0 & 0 \\ 0 & 0 & 0 & 0 \end{bmatrix} \in \boldsymbol{R}^{4\times 4} \tag{13}$$

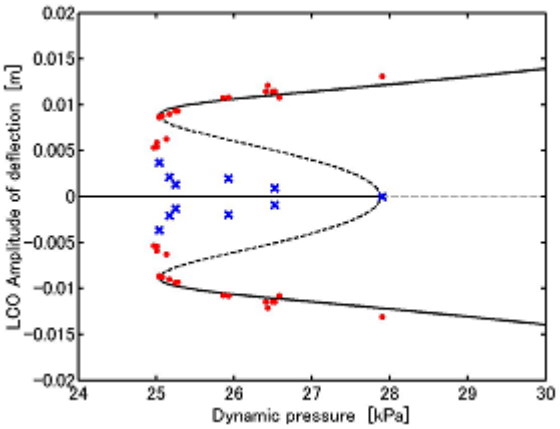

Fig. 9 Bifurcation diagram of analysis of the first mode.

If Fig. 9 is compared with Fig. 6, it turns out that Fig. 9 is a little closer to an experiment data.

Secondary, I added the nonlinear term to the second mode. The form of added nonlinear term is shown below.

$$\Delta\boldsymbol{A}_{INL}=\begin{bmatrix} 0 & 0 & 0 & 0 \\ 0 & (\beta_2 q_2^2+\gamma_2 q_2^4) & 0 & 0 \\ 0 & 0 & 0 & 0 \\ 0 & 0 & 0 & 0 \end{bmatrix} \in \boldsymbol{R}^{4\times 4} \tag{14}$$

It is very hard, however, to obtain the optimal model that fit the experimental data. I only have obtained a bifurcation diagram shown of the left hand side in Fig. 10.

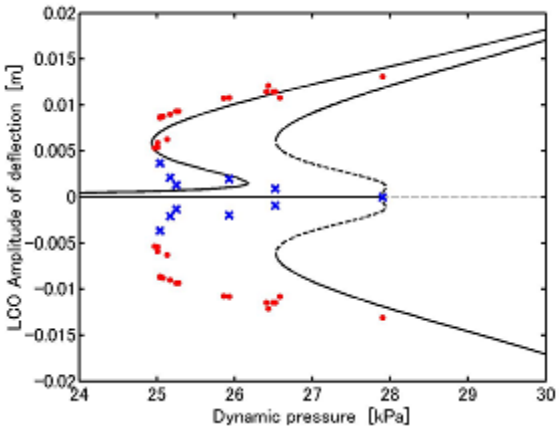

Fig. 10 Bifurcation diagram of analysis of the second mode.

Starting from the upper right corner, the continuation method can trace the bifurcation diagram rounding down at the saddle node, but on the way to the flutter point, it suddenly breaks down. I only could draw full bifurcation diagram as shown at the right hand side in Fig. 10, but bifurcation diagram differs from experiment data very much. I need to investigate why such an analysis result comes out.

6 Conclusions

The purpose of the present research is to reduce the discrepancy that exists in the previous model in the stability boundary region of bifurcation diagram between the mathematical model and the wind tunnel test data. I first work on a two-mode model. Suggested by Matsushita, I introduced the term $\beta_1 \dot{q}_1^2 + \gamma_1 \dot{q}_1^4$ in the first mode and the term $\beta_2 q_2^2 + \gamma_2 q_2^4$ in the second mode. I analyzed bifurcation characteristics of the new model by continuation method. The bifurcation characteristics of the model were able to improve greatly in the stability boundary region.

Intending to extend the two-mode model into four-mode model, I introduced the term $\beta_1 \dot{q}_1^2 + \gamma_1 \dot{q}_1^4$ in the first mode and the term $\beta_2 q_2^2 + \gamma_2 q_2^4$ in the second mode in the same way as the two-mode model. However, although I have obtained good results for the first mode, I have not yet obtained for the second mode. Therefore, investigation is still under way.

The parameters β_i's and γ_i's have been determined by the mathematical consideration, however, as suggested by Ref. [5], their physical meanings should be explored in future.

Acknowledgment

The author would like to appreciate Prof. Hiroshi Matsushita, University of Fukui, for his continuous supervision throughout this research and Mr. Takafumi Miyata of the same university for his support as well.

References

[1] Cunningham, A. M., Jr. Practical problem: airplanes. Chapter 3, *Unsteady transonic aerodynamics*, Nixon, D., ed., Progress in Astronautics and Aeronautics, 120, AIAA, pp. 75-132, 1989.

[2] Dowell, E. H. Nonlinear Aeroelasticity. *Flight-Vehicle Materials, Structures and Dynamics*, 5, Part II, Chapter 4, ASME, pp. 213 – 239, 1993.

[3] Schewe, G. and Deyhle, H. "Experiments on transonic flutter of a two-dimensional supercritical wing with emphasis on the non-linear effects." *Proceedings of the Royal Aeronautical Society Conference on "UNSTEADY AERODYNAMICS"*, 1996.

[4] Matsushita, H., Miyata, T., Christiansen, L. E. Lehn-Schioler, T and Mosekilde, E., "On the Nonlinear Dynamics Approach of Modeling the bifurcation for Transonic Limit Cycle Flutter", Proceedings of the 23rd International Congress of the Aeronautical Sciences, pp. 414.1-414.8, 2002

[5] Thomson, J. M. T., and Stewart, H. B., "Nonlinear Dynamics and Chaos", Second Edition, John Wiley & Sons, Ltd, 2002, pp. 58 – 61.